



1 **Dynamical Controls on Interannual ITCZ Variability over the** 2 **Indian Summer Monsoon Domain**

3 Priya Kumari^{1,2,*}, Preethi Bhaskar¹, Milind Mujumdar¹

4 ¹Centre for Climate Change Research (CCCR), Indian Institute of Tropical Meteorology,
5 Ministry of Earth Sciences (MoES), Pune, India

6 ²Department of Atmospheric and Space Science, Savitribai Phule Pune University, Pune, India

7 * Correspondence to: Priya Kumari (kumariPriya2626@gmail.com)

8

9

10 **Abstract**

11 The Intertropical Convergence Zone (ITCZ) is a narrow band of intense convection formed by the convergence
12 of tropical trade winds, leading to intense convection and precipitation. Its seasonal and interannual variations
13 have significant socio-economic impacts, particularly over the Indian subcontinent, where the shifts in ITCZ
14 position influence monsoon rainfall. Using long-term precipitation and atmospheric reanalysis data, this study
15 investigates the interannual variability of boreal summer ITCZ latitudes, quantified using multivariate
16 probabilistic approach, over the Indian region and its associated circulation changes. Extreme northward ITCZ
17 shift years are associated with enhanced convection, strengthened monsoon westerlies, and intensified ascent
18 leading to increased precipitation over the monsoon core zone along with poleward-displaced regional Hadley
19 circulation, while extreme southward shift exhibits opposite features. Large-scale climate modes such as the El
20 Niño–Southern Oscillation modulate tropical heating and circulation, influencing ITCZ position. Additionally, a
21 significant long-term northward shift of the ITCZ during 1940–2022 is identified, which is closely linked to
22 changes in moist static energy transport. A corresponding poleward shift of the meridional energy transport
23 indicates that this migration is driven by changes in atmospheric energy balance.

24

25 **1.Introduction**

26 The Intertropical Convergence Zone (ITCZ) is a narrow band along the equator spanning the globe, where the
27 tropical trade winds of the Northern and Southern Hemispheres converge (Sawyer, 1952; Zhang et al., 2021), and
28 is characterized by strong convergence, convection, and intense precipitation.

29 The ITCZ accounts for approximately 32 % of global precipitation and shapes climate and society in the tropics
30 (Byrne et al., 2018). Thus, understanding the variability and long-term changes in the ITCZ is crucial because its
31 position and intensity strongly regulate tropical rainfall, monsoon systems, and large-scale atmospheric
32 circulation. Factors affecting the ITCZ position and the dynamics behind its shifts are currently a key research
33 focus. Even small shifts in the ITCZ can lead to significant regional hydroclimatic impacts, including floods,
34 droughts, and food security risks for densely populated tropical regions.

35 Several studies have examined ITCZ variability on seasonal and interannual timescales using observations and
36 reanalysis data. The earlier studies include utilization of Highly Reflecting Cloud (HRC) dataset for computing
37 global as well as regional climatology of the ITCZ location and its variability (Waliser and Gautier 1993).



38 However, the HRC dataset was available for only a few years, which is insufficient to understand long-term
39 variability. Also, they talked about mean ITCZ latitude anomaly time series for different regions as well as
40 globally but did not discuss about trend. Interannual shifts of the zonal-mean ITCZ, computed using
41 precipitation, on global scale gave no significant global trend in the annual mean ITCZ position except for a
42 northward shift over the American sector and a southward shift over the western Pacific (Adam et al. 2016) while
43 pronounced year-to-year variability have been observed in ITCZ position and intensity across different ocean
44 basins (Liu et al. 2020). Other studies have investigated the structure and organization of ITCZ convection using
45 satellite and radio occultation observations, although these analyses are limited to relatively short time periods
46 (Basha et al. 2015). Previous studies have mostly investigated seasonal and interannual migrations of the ITCZ
47 either on a global scale or over the Atlantic and Pacific oceans (Žagar et al., 2011; Schneider et al. 2014;
48 Hohenegger, 2020). In monsoon regions, especially the Indian Summer monsoon, ITCZ variability is particularly
49 important, as seasonal rainfall is tightly linked to the position and migration of associated deep tropical convection
50 (Blandford, 1886; Gadgil, 2018). Growing evidence suggests that monsoon circulation is fundamentally driven
51 by diabatic heating associated with deep convection within the ITCZ, which generates large-scale atmospheric
52 responses (Hoskins and Rodwell, 1995; Chao, 2000; Chao and Chen, 2001). Thus, meridional shifts of the ITCZ
53 play a crucial role in regulating rainfall over monsoon regions in both hemispheres (Wang et al., 2014; Biasutti et
54 al., 2018).

55 Over the Indian monsoon domain, the ITCZ exhibits behavior distinct from that in the equatorial regions. While
56 precipitation variability near the equator is often associated with east–west displacements of the ITCZ, the Indian
57 summer monsoon is characterized by a pronounced north–south migration of the ITCZ (Goswami, 1997). Changes
58 in the meridional position of the ITCZ have been linked to major hydroclimatic variations. For instance, a
59 southward shift of the ITCZ from the Holocene thermal maximum to the onset of the Little Ice Age coincided
60 with a weakening of Indian summer monsoon rainfall (Schneider et al., 2014). Similarly, during the latter half of
61 the twentieth century, a southward migration of the ITCZ was associated with widespread droughts over North
62 China, South Asia, and the African Sahel (Biasutti and Giannini, 2006; Bollasina et al., 2011; Song et al., 2014;
63 Wodzicki and Rapp, 2016). In contrast, the strengthening of the Indian summer monsoon after 2002 has been
64 linked to a pronounced northward shift of the ITCZ over the Indian subcontinent (Hari et al., 2020).

65 Although many studies have identified the climatological location and structural patterns of the ITCZ, such as
66 northern, southern, and double ITCZ configurations, (Waliser and Gautier, 1993; Bain et al., 2011; Chen et al.,
67 2008) comparatively fewer studies have quantified its interannual variability, particularly in terms of changes in
68 position and convective intensity. As a result, the relationship between variability in ITCZ characteristics and the
69 associated large-scale circulation and hydrological cycle remains poorly understood (Wodzicki and Rapp, 2016).
70 This gap is especially critical over the Indian monsoon domain, where year-to-year variations in ITCZ latitude
71 strongly influence the spatial distribution and intensity of monsoon rainfall. The latitudinal position and extreme
72 shift of the ITCZ may be in response to the changes in the large-scale Walker circulation, but may also be a direct
73 consequence of the local SST anomalies which are themselves part of the global pattern of SST anomalies
74 associated with El Niño (Ju and Slingo, 1994). Thus, in this study this gap is addressed by examining the
75 interannual variability of the seasonal mean ITCZ location over the Indian monsoon domain and investigating the
76 associated large-scale circulation dynamics.



77 **2. Data and Methodology**

78

79 **2.1 Data**

80 The dataset used here, for the period 1940–2022, consists of monthly means of geopotential height, pressure
81 velocity, velocity potential and the zonal, specific humidity, temperature, meridional and vertical component of
82 wind at standard pressure levels, obtained from the ERA-Interim reanalysis (Hersbach et al., 2020) with grid size
83 of 0.25° latitude by 0.25° longitude. The domain considered in this study is the Indian summer monsoon region
84 (Equator–30°N, 60°–100°E). The rainfall anomalies are examined using the global precipitation dataset from CRU
85 (Climate Research Unit), with a horizontal resolution of 0.5° x 0.5° and available for the period 1901 to 2020
86 (Harris et al., 2020). Monthly SST data is derived from the Hadley Centre Global Sea Surface Temperature
87 (HadISST) dataset developed by Rayner et al. 2003 with a grid size of 1° latitude by 1° longitude.

88

89 **2.2 Methodology**

90 The ITCZ location is generally identified using single variable based metrics, but they are having large
91 discrepancy over the south Asian region. Mamalakis et al. (2021) used multivariate probabilistic tracking
92 framework to compute ITCZ location globally in terms of probability density function (pdf) based on precipitation
93 and outgoing longwave radiation (olr) data. A similar approach is followed by Kumari et al. (2026) and has
94 developed an index for ITCZ location by combining thermodynamical and dynamical parameters, namely
95 precipitation and meridional mass flux, respectively. This index is found to better represent the spatial variation
96 of ITCZ location over the south Asian domain during different phases of monsoon (Kumari et al. 2026).

97

98 In this study, the ITCZ location is computed following Kumari et al. (2026). For each season and sliding
99 longitudinal window, zonal-mean values of selected ITCZ-related variables are computed as functions of latitude.
100 At each latitude, variables are converted to marginal non-exceedance probabilities using rank-based empirical
101 cumulative distribution functions. These marginal probabilities are combined to estimate a joint non-exceedance
102 probability across all variables. Latitudes where the joint probability exceeds a prescribed threshold (0.85) are
103 identified as likely ITCZ locations. The distribution of these locations across all longitude windows is then
104 summarized using a probability density function, from which the seasonal mean ITCZ latitude is derived. The
105 analysis performed in this study is focused on the boreal summer monsoon season, i.e., JJAS (June-September).

106

107 To study the interannual variability of the ITCZ over the Indian monsoon region, we follow the same probabilistic
108 tracking approach (Kumari et al, 2025). First, the analysis is performed for the JJAS season for each individual
109 year. The longitude range is divided into overlapping windows of fixed width. For each longitude window and
110 year, zonal-mean of precipitation and mass flux are calculated as functions of latitude. At each latitude within a
111 window, the values of precipitation and mass flux are ranked relative to all other latitudes in the same window.
112 These ranks are then converted into marginal non-exceedance probabilities, which indicate how large the values
113 are compared to other latitudes. Next, the marginal probabilities of precipitation and mass flux are combined to
114 compute a joint non-exceedance probability at each latitude. Latitudes where this joint probability exceeds a
115 prescribed threshold are identified as potential ITCZ locations. For each longitude window, the latitude with the



116 maximum joint probability is selected as the ITCZ position. This procedure is repeated for all longitude windows,
117 and the ITCZ latitudes are averaged over longitude to obtain a single ITCZ latitude for each year. Repeating this
118 for all years produces a time series of ITCZ latitude, which is used to analyse its interannual variability.

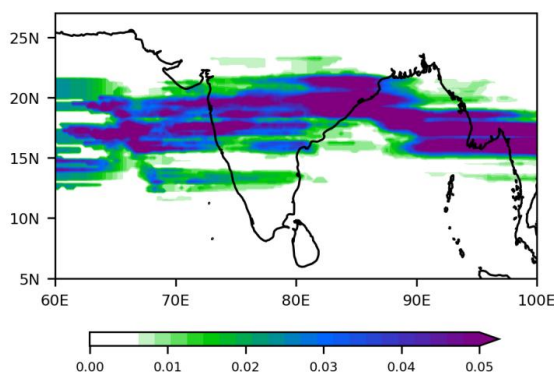
119 Moist Static Energy (MSE) is computed as follows:

120
$$\text{MSE} = gz + C_p T + Lq \quad \dots\dots\dots(1)$$

121 where g (acceleration due to gravity) = 9.8 ms^{-2} , z is geopotential height, C_p (Specific heat capacity at constant
122 pressure) = $1004 \text{ JK}^{-1}\text{Kg}^{-1}$, T is temperature, L (Latent heat of vaporisation) = $2.5 \times 10^6 \text{ JKg}^{-1}$ and q is specific
123 humidity.

124 **3.Results and Discussion**

125 To understand the preferred latitudinal position of the Intertropical Convergence Zone (ITCZ) during the monsoon
126 season, the PDF of the ITCZ latitude was computed for the JJAS period over the Indian monsoon domain. The
127 PDF provides information about the most frequently occurring latitudinal locations of the ITCZ. During the JJAS
128 season, highest PDF values (0.04–0.05) are observed between 15°N and 20°N, indicating that the ITCZ most
129 frequently resides within this latitude band during the monsoon season over the Indian monsoon domain as shown
130 in Figure 1. This latitude range corresponds to the active monsoon trough and regions of intense convection over
131 the Indian subcontinent. Thus, during the summer monsoon season, ITCZ remains predominantly north of the
132 equator, with negligible occurrence near the equator.



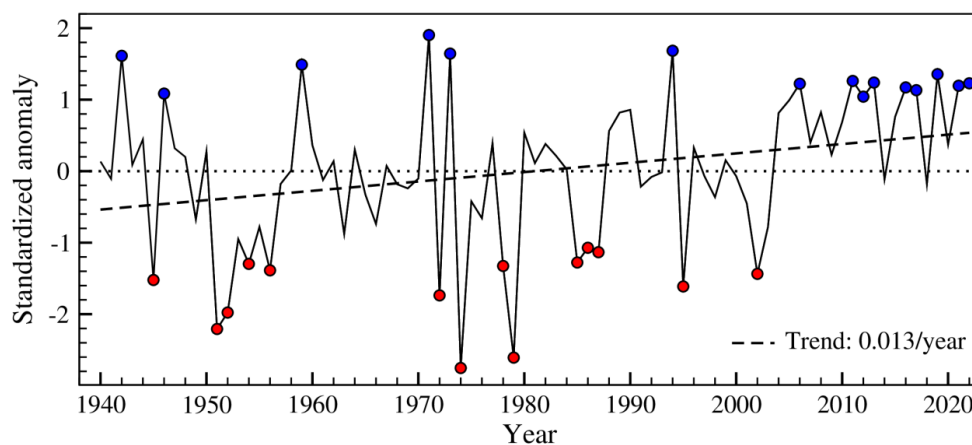
133

134 **Figure 1: Climatological ITCZ during JJAS season using Probability Density Function (PDF) for the**
135 **period 1940-2022.**

136



137 The JJAS mean ITCZ latitude during 1940–2022 over the South Asian monsoon region is located at 18.55° N,
138 with a standard deviation of 2.85 degrees, indicating substantial interannual variability in its position as shown in
139 Fig. 2.

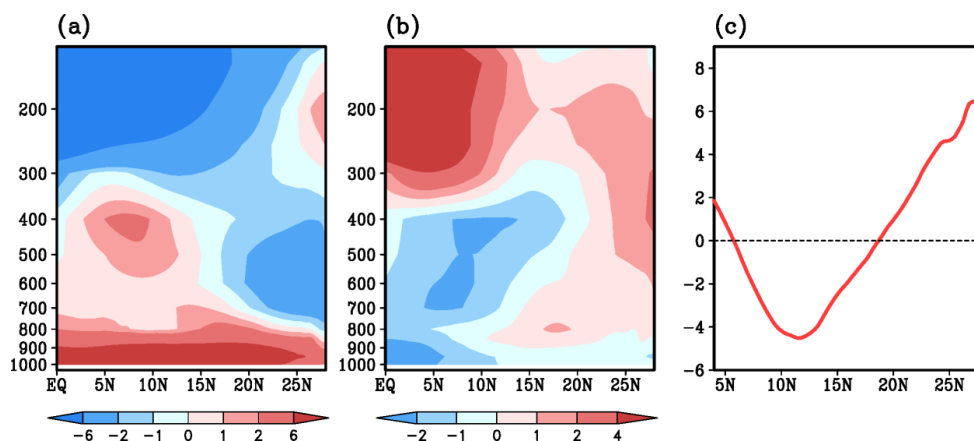


140

141 **Figure 2: Interannual variability of the JJAS mean ITCZ latitude expressed as standardized anomalies for**
142 **the period 1940-2022 over the region 60-100 °E. Green dots represent the years with extreme northward**
143 **shift and red dots represent years with extreme southward shift of ITCZ from its climatological mean. The**
144 **black dashed line shows linear trend.**

145 There is a significant increasing trend of approximately 0.013° latitude per year, implying a gradual northward
146 displacement of the ITCZ during JJAS season over the study period. These results are consistent with previous
147 studies that observed a northward propagation of ITCZ and strengthening of the Indian summer monsoon since
148 the early 2000s using reanalysis dataset (Hari et al, 2020). Similarly, a satellite-based analysis finds the tropical
149 convection band contracting and moving toward the Northern Hemisphere at ~30 km/decade over land (Aumann et
150 al, 2024). Moreover, CMIP6 projections also point to a robust northward shift of ITCZ in the Eurasian (20°E–130°E)
151 sector under 21st century warming (Mamalakis et al, 2021). The proposed possible drivers of this shift include
152 enhanced Northern Hemisphere (and Indian Ocean) warming and rising sea-surface temperature (SST) asymmetry
153 (Weller et al, 2014; Sun et al , 2024) along with reduced aerosol cooling over South Asia (Hari et al, 2020).

154 The position of the ITCZ is fundamentally controlled by the large-scale energy balance. It lies at the foot of the
155 ascending branch of the tropical Hadley circulation close to where the near surface zonal mean meridional Moist
156 static energy (MSE) flux vanishes or changes sign. (Adam et al, 2016). MSE is a combination of internal, latent,
157 and potential energy, (Equation (1)) which together govern large-scale circulation and energy transport and is a
158 direct measure of convection. A higher value of MSE represents higher energy to carry the moisture upwards,
159 which leads to condensation of the moisture and hence rainfall (Polcher,1995).



160

161

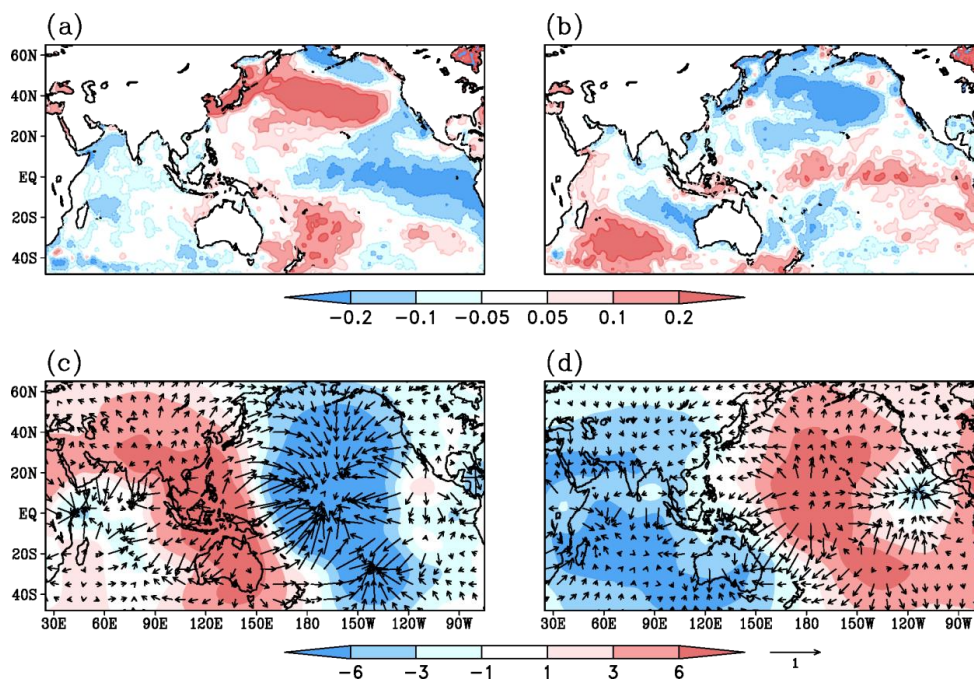
162 **Figure 3: (a) Climatological Vertical profile of zonally averaged meridional MSE flux ($\times 10^5$ J/m/s) (b)**
 163 **Linear trend of the zonal mean meridional MSE flux ($\times 10^3$ J/m/s/year) and (c) Linear trend of the vertically**
 164 **integrated zonally averaged meridional MSE flux ($\times 10^6$ J/m/s/year) over the period 1940-2022 for JJAS**
 165 **season.**

166 The climatological structure of meridional MSE flux over the 60°–100°E domain during JJAS season (Fig
 167 3a) exhibits a well-defined overturning circulation, with strong northward transport in the lower troposphere
 168 (~850–1000 hPa) and a compensating southward return flow aloft in the upper troposphere (~100–300 hPa),
 169 indicating that energy is exported away from the ITCZ in the upper branch. This vertical dipole structure reflects
 170 a thermally direct circulation associated with the monsoon Hadley cell, where energy is carried poleward near the
 171 surface and returned equatorward aloft. Figure 3b shows the trend in MSE flux over the study area. The lower
 172 troposphere (700–900 hPa) shows a marked increase in northward MSE flux north of 15°N, highlighting
 173 strengthened energy transport into higher latitudes. In contrast, the mid-troposphere (400–700 hPa) exhibits a
 174 significant decrease in MSE flux south of about 10–15°N, indicating a reduction in energy transport in the
 175 equatorial and southern regions. The upper troposphere (100–300 hPa) shows a broad positive trend, suggesting
 176 enhanced export of energy aloft. Together, these features form a clear meridional dipole pattern, characterized by
 177 decreasing transport to the south and increasing transport to the north, which indicates a poleward shift of the
 178 atmospheric energy transport. This vertically coherent structure reflects a reorganization of the large-scale
 179 monsoon Hadley circulation and implies a northward displacement of the energy convergence zone. Furthermore,
 180 the column integrated MSE flux trend (Fig 3c) is positive (negative) north (south) of 18°N. Positive trend implies
 181 increasing northward transport whereas negative trend means decrease in northward transport. Thus, northward
 182 energy transport is increasing north of 18°N which in turn shifts ITCZ northward whereas south of 18°N the
 183 northward transport is decreasing. This is a dynamically consistent explanation for the observed poleward
 184 migration of the ITCZ over the Indian monsoon domain.



185 Despite this long-term poleward shift, pronounced year-to-year fluctuations remain a dominant feature. Years
186 exceeding +1 standard deviation (SD) are classified as extreme northward ITCZ shift, while years with anomalies
187 below -1 SD are categorised as extreme southward ITCZ shift from their climatological mean position. Based on
188 the standardized JJAS ITCZ latitude anomalies, 16 years – 1942, 1946, 1959, 1971, 1973, 1994, 2005, 2006, 2011,
189 2012, 2013, 2016, 2017, 2019, 2021, and 2022 – are classified as extreme northward shift of ITCZ while 14 years
190 – 1945, 1951, 1952, 1954, 1956, 1972, 1974, 1978, 1979, 1985, 1986, 1987, 1995 and 2002 – are classified as
191 extreme southward shift of ITCZ. The figure also indicates pronounced oscillations in ITCZ position prior to
192 1970, with extreme shifts occurring both northward and southward. During the period 1970–2000, the ITCZ
193 exhibited predominantly extreme southward shifts. In contrast, after 2000, most years were characterized by
194 pronounced northward shifts of the ITCZ. The extreme years provide a basis for composite analysis, allowing
195 isolation of circulation and thermodynamic anomalies associated with extreme ITCZ shifts during the JJAS
196 season.

197 In the northward shift composite (Fig.4a), warm SST anomalies across much of the tropical Indian ocean including
198 Arabian sea and Bay of Bengal is observed. Warm anomalies are also evident in the Western and central Pacific
199 whereas relatively cool anomalies are observed in eastern equatorial Pacific. This pattern resembles La-Nina like
200 conditions (Philander, 1990; McPhaden et al, 2006). In contrast, southward ITCZ shift composite (Fig.4b)
201 coincide with widespread cooling over the Indian Ocean and warming in the central-eastern Pacific, consistent
202 with El-Nino like condition (Philander, 1990; Trenberth, 1997; McPhaden et al, 2006).



203



204 **Figure 4: Composite SST anomaly (°C) for (a) northward and (b) southward shift of ITCZ and Velocity**
205 **Potential anomaly (s^{-1}) for (c) northward and (d) southward shift of ITCZ during JJAS season over the**
206 **Indian region.**

207

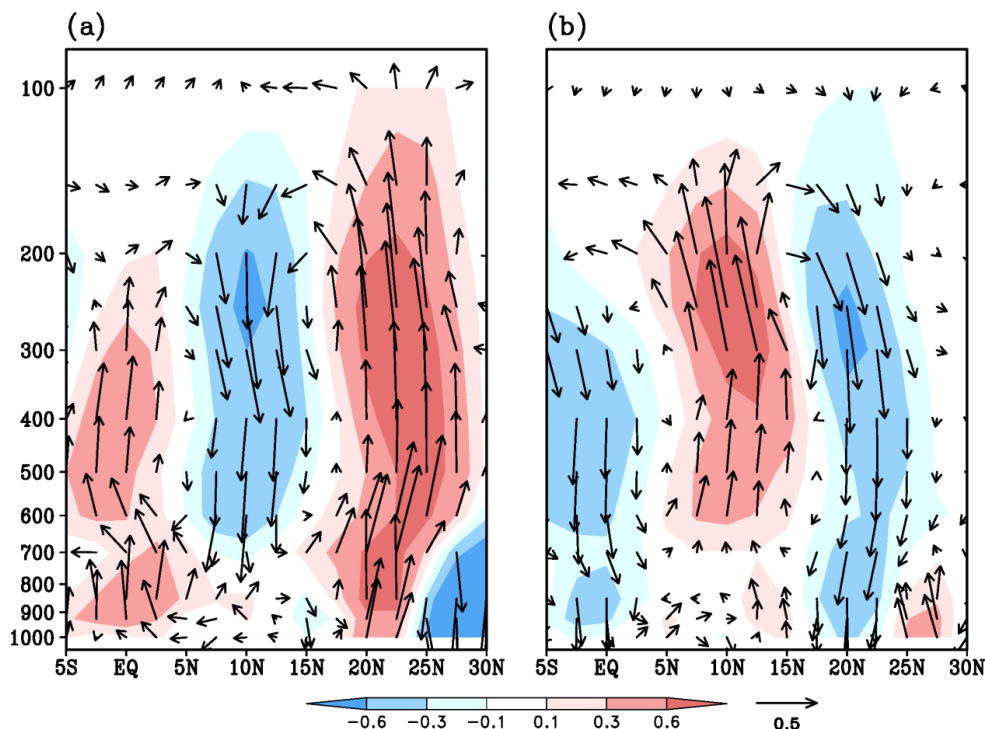
208 The velocity potential (VP) composite anomalies at 200 hPa are dynamically consistent with the underlying SST
209 pattern. During the northward ITCZ shift (Figure 4c), positive VP anomalies dominate over the Indian Ocean and
210 the Indian subcontinent, indicating enhanced upper-tropospheric divergence and large-scale ascent over the
211 monsoon region, while negative VP anomalies over the central eastern equatorial Pacific reflect upper-level
212 convergence and suppressed convection there. This zonal contrast in VP signifies a westward-displaced Walker
213 circulation, favoring enhanced convective activity and hence an anomalous increase in diabatic heating over the
214 Indian sector. In contrast, the composite analysis during the southward ITCZ shift is characterized by strong
215 positive VP anomalies over the central–eastern equatorial Pacific and negative VP anomalies over the Indian
216 Ocean and adjoining land areas, indicating a reversal of the zonal overturning circulation with enhanced ascent
217 over the Pacific and anomalous subsidence over the Indian landmass and adjoining seas.

218 The Indian summer monsoon consists of both planetary-scale and regional-scale circulation components, with the
219 regional circulation playing a dominant role in governing monsoon rainfall variability. During boreal summer, the
220 ITCZ shifts northward from its wintertime equatorial position to about 15–20°N over the Indian region, while
221 remaining closer to the equator over the western Pacific. This latitudinal displacement creates a strong zonally
222 asymmetric off-equatorial heat source over India near 20°N. According to Gill's (1980) theoretical framework,
223 such off-equatorial heating preferentially generates a strong regional Hadley circulation. Being a convectively
224 coupled system, the seasonal mean rainfall is strongly correlated with the regional Hadley circulation associated
225 with rising vertical motions along the regional ITCZ (Goswami et al, 1999; Bajrang et al, 2023). As a result, the
226 Indian summer monsoon can be viewed as a superposition of a regional Hadley circulation driven by monsoon
227 heating over ~15–20°N, and a planetary-scale Walker circulation associated with equatorial heating, particularly
228 over the Pacific.

229 The composite anomalies of the local Hadley circulation further illustrate how this dynamical framework responds
230 during ITCZ shifts. During northward ITCZ shift years (Fig.5a), anomalous ascent is enhanced over ~10–25°N
231 and extends through much of the troposphere, accompanied by compensating subsidence over lower latitudes.
232 This pattern indicates a strengthened and poleward-displaced regional Hadley circulation in response to the
233 increased diabatic heating due to the westward shift of the ascending branch of the Walker cell during La Niña.



234

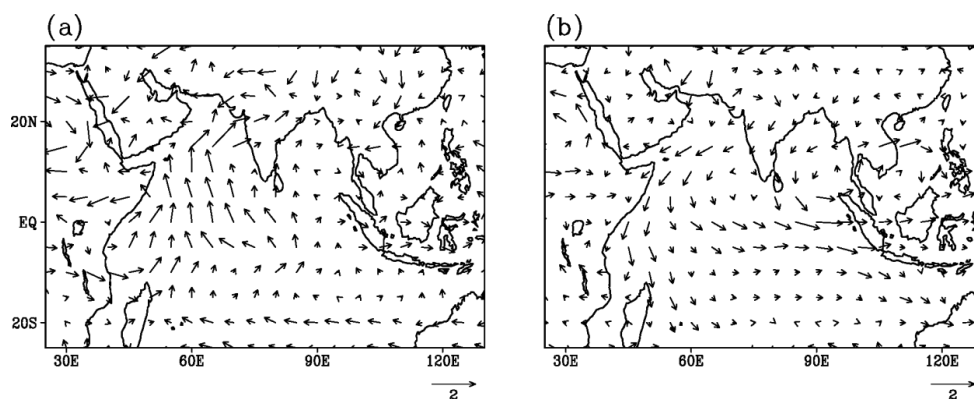


235

236 **Figure 5: Local Hadley cell anomaly during JJAS season for years with (a) northward (left) and (b)**
 237 **southward shift (right) composites.**

238 In contrast, during southward ITCZ shift years (Fig 5b), anomalous ascent is confined closer to the equator, while
 239 pronounced subsidence dominates over nearly 17-25°N, reflecting a weakened and equatorward-shifted local
 240 Hadley circulation. These results demonstrate that interannual ITCZ shifts over the Indian monsoon domain arise
 241 from a coupled adjustment of zonal (Walker) and meridional (regional Hadley) overturning circulations, in which
 242 Walker circulation anomalies modulate the longitudinal distribution of heating, while the regional Hadley
 243 circulation determines the meridional position of the ITCZ.

244 Consistent with these vertical overturning anomalies, the composite analysis of 850-hPa wind (Figure 6), also
 245 known as southwesterly flow which is a dominant source of moisture transport for South Asian summer monsoon
 246 region (Preethi et al 2017), reveals distinct low-level circulation signatures associated with each ITCZ shift phase.
 247 The southwesterly flow over Indian Ocean is a dominant source of moisture transport for South Asian summer
 248 monsoon region. During northward ITCZ shift years (Figure 6a), anomalous southwesterlies over the Arabian Sea
 249 and strengthened cross-equatorial flow from the southern Indian Ocean converge over the Indian subcontinent,
 250 particularly north of 20°N. This enhanced low-level convergence supports increased moisture transport and leads
 251 to deep convection over northern latitudes, anchoring the ascending branch of the regional Hadley circulation
 252 poleward of its climatological position.



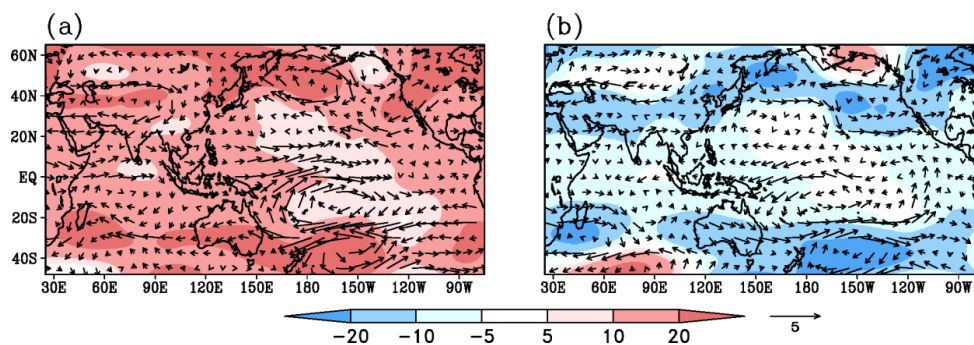
253

254 **Figure 6: Wind anomalies at 850 hPa during JJAS season for years with northward (left) and southward**
 255 **shift (right) composites.**

256 In contrast, southward ITCZ shift years (Figure 6b) are characterized by weakened monsoon westerlies and
 257 anomalous northerly to northeasterly flow over the Indian region, leading to reduced moisture influx and
 258 diminished low-level convergence over land. As a result, convergence and ascent remain confined closer to the
 259 equator, favoring an equatorward displacement of the ITCZ.

260 These contrasting low-level wind patterns indicate that it is not the basin-wide strength of convergence but the
 261 meridional relocation of the convergence maximum that governs ITCZ shifts. By modulating the latitude of
 262 diabatic heating through changes in moisture transport and convergence, the low-level circulation plays a crucial
 263 role in translating large-scale ENSO forcing into regional ITCZ and monsoon variability over the Indian domain.

264 Following the low-level circulation anomalies, the upper-tropospheric response is further illustrated by the 200-
 265 hPa geopotential height (GPH) composite anomalies (Fig. 7).



266

267 **Figure 7: Geopotential height anomalies at 200 hPa during JJAS season for years with northward (left)**
 268 **and southward shift (right) composites represented by shading and vector arrows represent composite wind**
 269 **anomaly at 200hPa.**

270

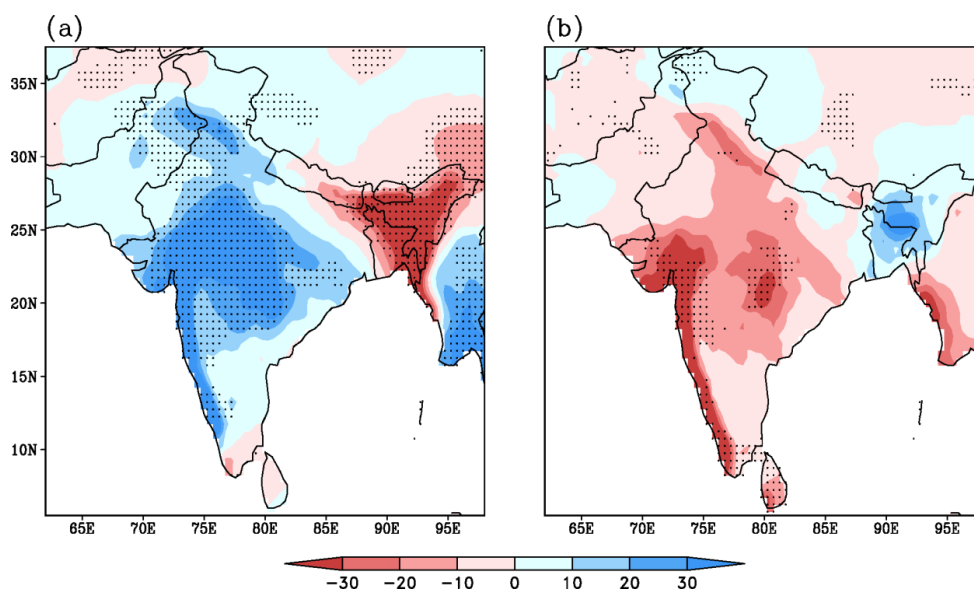


271 During northward ITCZ shift years (Fig. 7a), positive GPH anomalies dominate over the Indian subcontinent and
272 adjacent regions, indicating a warm upper-tropospheric column associated with enhanced diabatic heating and
273 deep convection over northern latitudes. This upper-level height rise is consistent with strengthened divergent
274 outflow at 200 hPa and reflects the development of an anomalous anticyclonic circulation aloft, a canonical
275 response to intensified monsoon heating. Such an upper-tropospheric mass redistribution supports sustained
276 ascent in the northern branch of the regional Hadley circulation, thereby reinforcing the poleward displacement
277 of the ITCZ. In contrast, southward ITCZ shift years (Fig. 7b) exhibit negative GPH anomalies over the Indian
278 region, indicative of a cooler tropospheric column and suppressed latent heat release. The weakened upper-level
279 anticyclonic response and enhanced convergence aloft are consistent with reduced deep convection and
280 diminished monsoon heating. As a result, the ascending branch of the regional Hadley circulation shifts
281 equatorward, confining convection closer to the equator and favoring a southward displacement of the ITCZ.

282 Taken together, the low-level wind anomalies, upper-level velocity potential, and geopotential height responses
283 provide a dynamically consistent picture in which ENSO-driven modulation of tropical heating reorganizes both
284 the lower- and upper-tropospheric circulation, leading to systematic shifts in the regional Hadley circulation and
285 the meridional position of the ITCZ over the Indian region.

286 During northward ITCZ shift years (Fig. 8a), significant enhanced precipitation anomalies are concentrated over
287 monsoon core zone and northern India (~15–25°N), while negative anomalies appear to the south, indicating a
288 poleward displacement of the convective heating maximum. This northward relocation of latent heat release
289 strengthens ascent in the northern branch of the local Hadley circulation, reinforcing the poleward shift of the
290 ITCZ.

291



292



293 **Figure 8: Precipitation anomalies (mm day^{-1}) for the JJAS season based on CRU dataset for the northward**
294 **and southward shift composite. The hatches represent significant values at the 95% confidence level.**

295

296 In contrast, southward ITCZ shift years (Fig. 8b) exhibit a significant suppression of rainfall over much monsoon
297 core zone, reflecting an equatorward displacement of deep convection and associated heating. Thus, the
298 precipitation composite anomalies further confirm the heat-driven nature of the ITCZ shifts over the Indian region.

299 4. Conclusion

300 This study demonstrates a clear northward shift in the ITCZ location over the Indian monsoon domain during the
301 JJAS season. This shift is linked to changes in moist static energy transport, with more energy moving toward
302 higher latitudes. This indicates that changes in atmospheric energy balance are driving the movement of the ITCZ
303 over the Indian monsoon region.

304 The interannual time series highlights years with extreme latitudinal shifts of the ITCZ over the Indian monsoon
305 domain. Before 1970, the ITCZ exhibited strong oscillations with both extreme northward and southward shifts.
306 During 1970–2000, extreme southward shifts dominated, whereas after 2000, the ITCZ predominantly showed
307 extreme northward shifts.

308 Moreover, interannual shifts of the ITCZ over the Indian region during the boreal summer are primarily governed
309 by the coupled adjustment of the zonal (Walker) and meridional (local Hadley) overturning circulations, rather
310 than by a direct local Walker subsidence over India. ENSO-related modulation of the Walker circulation alters
311 the longitudinal distribution of tropical convection and upper-tropospheric divergence, leading to a zonally
312 asymmetric heating pattern with a pronounced off-equatorial maximum over the Indian region. Consistent with
313 the Gill (1980) framework, this asymmetric heating excites a strong local Hadley circulation, whose latitude of
314 maximum ascent determines the meridional position of the ITCZ. During northward ITCZ shift years, enhanced
315 convective heating over $\sim 15\text{--}25^\circ\text{N}$ strengthens low-level convergence, cross-equatorial monsoon flow, and upper-
316 level divergence, resulting in an intensified and poleward-displaced local Hadley cell. In contrast, southward shift
317 years are characterized by weakened monsoon westerlies, reduced upper-level divergence, and an equatorward
318 shift of ascent, leading to a southward displacement of the ITCZ. These circulation changes are coherently
319 reflected in the composites of velocity potential, geopotential height, low-level winds, and precipitation
320 anomalies, underscoring the dynamically consistent response of the atmosphere to changes in the spatial structure
321 of monsoon heating.

322 Overall, the results highlight that ITCZ variability over the Indian monsoon domain arises from a heat-driven shift
323 of the regional Hadley circulation, modulated remotely by ENSO-induced changes in the Walker circulation. This
324 coupled zonal–meridional framework provides a physically consistent explanation for ITCZ shifts and emphasizes
325 the central role of regional-scale circulation in shaping Indian summer monsoon variability. Future studies can
326 employ climate model simulations to further investigate the mechanisms controlling ITCZ variability over the
327 Indian monsoon domain.

328 **Author contributions**



329 P.K. and P.B. conceived the study. P.K. performed the data analysis and wrote the original drafts of the paper and
330 the methods section. P.K. and P.B. generated the figures. M.M. supervised the project. All authors reviewed and
331 approved the final manuscript.

332 **Competing interests**

333 The authors declare that they have no known competing financial interests or personal relationships that could
334 have appeared to influence the work reported in this paper.

335 **Disclaimer**

336 Publisher's note: Copernicus Publications remains neutral with regard to jurisdictional claims made in the text,
337 published maps, institutional affiliations, or any other geographical representation in this paper. While Copernicus
338 Publications makes every effort to include appropriate place names, the final responsibility lies with the authors.

339 **Acknowledgements**

340 We sincerely thank Director, Indian Institute of Tropical Meteorology (IITM, India) and Project Director, Centre
341 for Climate Change Research (CCCR at IITM) for all the support during the research study. This work is a part
342 of the Ph.D. Thesis of the first author.

343 **Financial support**

344 This work has been supported by IITM. IITM is fully funded by the Ministry of Earth Sciences, Government of
345 India.

346 **Data Availability Statement**

347 Data used here can be downloaded from the following: CRU (<https://crudata.uea.ac.uk/cru/data/hrg/>), ERA5
348 (<https://cds.climate.copernicus.eu/datasets>), and HadISST
349 (<https://www.metoffice.gov.uk/hadobs/hadisst/data/download.html>).

350

351 **References**

352 Adam, O., Bischoff, T., Schneider, T. (2016). Seasonal and interannual variations of the energy flux equator and
353 ITCZ. Part I: Zonally averaged ITCZ position. *J. Clim.* 29, 3219–3230. <https://doi.org/10.1175/JCLI-D-15-0512.1>.

355 Basha, G., Kishore, P., Ratnam, M. V., Ouarda, T. B. M. J., Velicogna, I., and Sutterly, T. (2015). Vertical and
356 latitudinal variation of the intertropical convergence zone derived using GPS radio occultation measurements,
357 *Remote Sens. Environ.*, 163, 262–269, <https://doi.org/10.1016/j.rse.2015.03.024>

358 Biasutti M, Giannini A (2006) Robust Sahel drying in response to late 20th century forcings. *Geophys Res Lett*
359 33:L11706

360 Blandford, H. F. (1886). *Rainfall of India; monsoon monograph*. India Meteorological Department, 3, 658.

361 Bollasina MA, Ming Y, Ramaswamy V (2011) Anthropogenic aerosols and the weakening of the South Asian
362 summer monsoon. *Science* 334 (6055):502–505.



- 363 Byrne, M.P., Pendergrass, A.G., Rapp, A.D., Wodzicki, K.R. (2018). Response of the intertropical convergence
364 zone to climate change: location, width, and strength. *Curr. Clim. Chang. Rep.* 4, 355–370.
- 365 C. Bajrang, R. Attada, B.N. Goswami (2023). Possible factors for the recent changes in frequency of central
366 Indian Summer Monsoon precipitation extremes during 2005–2020. *NPJ. Clim. Atmos. Sci.*,6. [10.1038/s41612-](https://doi.org/10.1038/s41612-023-00450-y)
367 [023-00450-y](https://doi.org/10.1038/s41612-023-00450-y)
368
- 369 Chao, W. C. (2000), Multi quasi equilibria of the ITCZ and the origin of monsoon onset, *J. Atmos. Sci.*, 57, 641-
370 651.
- 371 Chao, W. C., Chen, B. (2001). The origin of monsoons. *J. Atmos Sci.* 58, 3497-3507.
- 372 Chen, B., X. Lin, and J. T. Bacmeister (2008), Frequency distribution of daily ITCZ patterns over the western-
373 central Pacific, *J. Clim.*, 21, 4207–4222.
- 374 Gadgil, S. (2018). The monsoon system: Land–sea breeze or the ITCZ? *J. Earth Syst. Sci.* 127.
375 <https://doi.org/10.1007/s12040-017-0916-x>.
- 376 Gill, A. E. (1980). Some simple solutions for heat-induced tropical circulation. *Q. J. R. Meteorol. Soc.* 106, 447–
377 462.
- 378 Goswami, B.N. Chaos and predictability of the Indian summer monsoon. *Pramana - J Phys* 48, 719–736 (1997).
379 <https://doi.org/10.1007/BF02845671>
- 380 Goswami, B.N., Krishnamurthy, V., Annamalai, H. (1999). A broad-scale circulation index for the interannual
381 variability of the Indian summer monsoon. *Q. J. R. Meteorol. Soc.* 125 (554), 611–633.
382 <https://doi.org/10.1002/qj.49712555412>.
- 383 Harris, I., Osborn, T. J., Jones, P., & Lister, D. (2020). Version 4 of the CRU TS monthly high-resolution gridded
384 multivariate climate dataset. *Scientific data*, 7(1), 109.
- 385 Hersbach, H., Bell, B., Berrisford, P., Hirahara, S., Horányi, A., Muñoz-Sabater, J., Nicolas, J., Peubey, C.,
386 2020. The ERA5 global reanalysis. *Q. J. R. Meteorol. Soc.* 146 (730), 1999–2049. <https://doi.org/10.1002/qj.3803>.
- 387 Hohenegger C, Jakob C. (2020). A relationship between ITCZ organization and subtropical humidity. *Geophys.*
388 *Res. Lett.* 47:e2020GL088515.
- 389 Ju, J. and Slingo, J. (1995), The Asian summer monsoon and ENSO. *Q.J.R. Meteorol. Soc.*, 121: 1133-
390 1168. <https://doi.org/10.1002/qj.49712152509>
- 391 Kumari, P., Preethi, B., & Mujumdar, M. (2025). Climatological characteristics of ITCZ over the South Asian
392 monsoon domain: Using multivariate probabilistic approach. *Atmospheric Research*, 108709.
- 393 Liu, C., Liao, X., Qiu, J., Yang, Y., Feng, X., Allan, R.P., Cao, N., Long, J., Xu, J. (2020). Observed variability of
394 intertropical convergence zone over 1998–2018. *Environ. Res. Lett.* <https://doi.org/10.1088/1748-9326/aba033>.
- 395 Mamalaklis, A., Randerson, J.T., Yu, J.Y., 2021. Zonally contrasting shifts of the tropical rain belt in response to
396 climate change. *Nat. Clim. Chang.* 11, 143–151. <https://doi.org/10.1038/s41558-020-00963-x>.
- 397 Preethi B, Mujumdar M, Kripalani RH, Prabhu A, Krishnan R. (2017). Recent trends and tele-connections among
398 South and East Asian summer monsoons in a warming environment. *Clim Dyn* 48:2489–2505
- 399 Rayner, N. A., Parker, D. E., Horton, E. B., Folland, C. K., Alexander, L. V., Rowell, D. P., ... & Kaplan, A. J. J.
400 O. G. R. A. (2003). Global analyses of sea surface temperature, sea ice, and night marine air temperature since
401 the late nineteenth century. *Journal of Geophysical Research: Atmospheres*, 108(D14)
- 402 Rodwell, M.J., Hoskins, B.J. (1995). A model of the Asian summer monsoon. Part II: cross- equatorial flow and
403 PV behavior. *J. Atmos. Sci.* 52 (9), 1341–1356. [https://doi.org/10.1175/1520-](https://doi.org/10.1175/1520-0469(1995)052%3C1341:AMOTAS%3E2.0.CO;2)
404 [0469\(1995\)052%3C1341:AMOTAS%3E2.0.CO;2](https://doi.org/10.1175/1520-0469(1995)052%3C1341:AMOTAS%3E2.0.CO;2).



- 405 Sawyer, J.S. (1952). Memorandum on the International Front. Meteor. Rept. No. 10, Meteorological Office,
406 London, 1-14.
- 407 Schneider, T., Bischoff, T. & Haug, G. H. (2014) Migrations and dynamics of the intertropical convergence
408 zone. *Nature* **513**, 45–53.
- 409 Song, F., T.Zhou, and Y.Qian (2014), Responses of East Asian summer monsoon to natural and anthropogenic
410 forcings in the 17 latest CMIP5 models, *Geophys. Res. Lett.*, 41, 596–603, doi:10.1002/2013GL058705.
- 411 Wang, P. X., Wang, B., Cheng, H., Fasullo, J., Guo, Z. T., Kiefer, T., and Liu, Z. Y.: The global monsoon across
412 timescales: coherent variability of regional monsoons, *Clim. Past*, 10, 2007–2052, [https://doi.org/10.5194/cp-10-](https://doi.org/10.5194/cp-10-2007-2014)
413 [2007-2014](https://doi.org/10.5194/cp-10-2007-2014), 2014.
- 414 Wodzicki, K. R. & Rapp, A. D. Long-term characterization of the Pacific ITCZ using TRMM, GPCP, and ERA-
415 Interim. *J. Geophys. Res. Atmos.* **121**, 3153–3170 (2016).
- 416 Žagar, N., G. Skok, and J. Tribbia (2011), Climatology of the ITCZ derived from ERA Interim reanalyses, *J.*
417 *Geophys. Res.*, 116, D15103, doi:10.1029/2011JD015695.
- 418 Zhang, H., Ma, X., Zhao, S. (2021). Advances in research on the ITCZ: mean position, model bias, and
419 anthropogenic aerosol influences. *J. Meteorol. Res.* 35 (5), 729–742. [https://doi.org/10.1007/S13351-021-0203-](https://doi.org/10.1007/S13351-021-0203-2)
420 [2](https://doi.org/10.1007/S13351-021-0203-2).
- 421
- 422